ASEAN Engineering Journal

Full Paper

A PARAMETRIC STUDY ON LATERAL LOAD BEHAVIOR OF INTERIOR FLAT PLATE - COLUMN CONNECTIONS

Hizbawi Sisay, Temesgen Wondimu

Department of Civil Engineering, Addis Ababa science and Technology University, Addis Ababa, Ethiopia

Article history
Received
30 May 2021
Received in revised form
07 November 2021
Accepted
01 January 2022
Published online
31 May 2022

*Corresponding author
hizbawi.sisay@aastu.edu.et

Graphical abstract

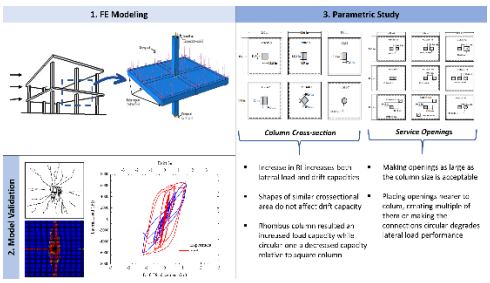

Abstract

Reinforced concrete flat plate structures have been used in the construction industry since the start of the 20th century due to their architectural flexibility and economy. Through the years the structures were mainly designed to carry gravity loads due to their high flexibility in their connection regions. Unfortunately, these structures may sometimes be subjected to lateral and gravity loads due to unexpected natural phenomenon such as earthquakes. The information on behavior of these structures under such loading condition is limited. This paper presents parametric study on isolated flat plate connections under combined gravity and lateral loads using a non-linear finite element analysis. The numerical model for the connections was developed using ABAQUS in which plasticity model for concrete and an elastic-plastic model for steel reinforcement was employed. The model was validated with an experimental test, conducted by other researchers, of similar loading condition. The results of parametric study on the effect of column geometry and service openings adjacent to the column are presented. Among the parameters, the effect of column geometry was found to have significant effects on the connection behavior.

Keywords: Column geometry, Cyclic lateral loads, Finite element analysis, Flat plate connection, Service openings

1.0 INTRODUCTION

It is generally recognized that reinforced concrete flat plate systems are not efficient in resisting lateral loads though they are preferred as a gravity load supporting systems for their pleasing appearance and economy [1]. As a result of their weakness in energy dissipation capacity and lateral stiffness, they are usually supplemented by other systems such as structural shear walls in the event of lateral loading [2]. However, in the event of past natural events such as earthquakes the structures designed for mere purpose of carrying gravity loads have been seen to led to catastrophic damages [3]–[5]. The failures are primarily due to punching shear in the connection regions. Under such circumstances or in need of supplementary lateral load systems, it becomes apparent that understanding the contribution of the flat plate framework to lateral resistance along with its traditional role as a vertical load-carrying system is important.

The lateral load behavior of RC flat plate column (FPC) connections both in combination with and without gravity loads have been the subject of several researches over the past few decades. Experimental contributions to the subject were made by many researchers subjecting flat plate specimens to cyclic horizontal loads [6]–[14]. The major variables in these tests were concrete strength, longitudinal reinforcement ratio, support conditions, the type and arrangement of shear reinforcement, lateral loading history and level of gravity load. In comprehension, the studies have reported that horizontal loading will limit the horizontal drift capacity and ductility of flat plate connections and these will be severed by the addition of gravity loads. These types of structures showed limited horizontal drift capacity and ductility under horizontal loading, especially if it is combined with gravity loads. In addition, supplementing the connections with different shear reinforcements can improve their lateral load resistance even if the level of the effect is different for each type. However, providing a shear reinforcement is not

always easy and thus this paper is limited to plates without transverse reinforcement. Other variables considered in these types of tests were the supporting column rectangularity [15]–[17] and arrangement and size of service openings on the plate surface [18]–[21].

Though the behavior of flat plate connections under horizontal cyclic reversals has been a subject of several experiments, it is not yet sufficiently understood due to the need for the consideration of large number of variables. So, all aspects and combination of parameters as well as mechanisms to prevent failure were not accessed for the obvious cost and time needs. One approach is using finite element analysis (FEA) given that it is a promising approach that could provide a platform to study numerous variables in one setting and reduce the resources needed in experiments but it needs some critical phenomenon, the punching shear failure in this case, to be reproduced. Besides, such a simulation has been used in many numerical studies using various elements and proved to be applicable to such type of studies [22]–[24].

This paper presents the results of a FEA performed on isolated flat plate-column connections, originally referred from literature and modified for parametric study using ABAQUS software [25]. Connections having different service openings, columns with varying rectangularity ratios and different sizes were loaded vertically and laterally to contribute for the database on the subject. The concrete is modelled with the concrete damaged plasticity model (CDPM) incorporated in the software.

2.0 MODEL VALIDATION

Experimental Background for Validation

An experimental test performed by Pan and Moehle [26] have been used in order to validate the slab numerical model described and developed in the next section of this paper. In the experimental test, reduced scale models of RC plate-to-column connection were tested.

The specimens tested were connections which were part of a continuous plate column system. Slab dimensions were 3962 × 3962 × 122 mm and the column had a square cross-section of 274 × 274 mm. The height of the column measured from the top and the bottom faces of the slab was 914 mm. The materials specified for the test specimen were those commonly used in construction practice. The concrete specified for the slab and column was 28 MPa normal weight concrete. The reinforcement was a typical one having yield strength of 414 MPa. The slab had steel top and bottom meshes, both built with No. 3 (10 mm) deformed bars. Continuous bottom bars were placed directly over the column to prevent progressive collapse. The column was reinforced with No. 7 (22 mm) deformed main bars while the stirrups were No. 2 (6.4 mm) plain bars and the plate was simply supported along the edges, spanning 3660 mm in both horizontal directions.

The slab was tested under a static vertical gravity load applied on the slab top and a lateral reversed cyclic loading applied through the column until failure, in this particular case, by punching shear or flexure. The test was performed with displacement-controlled history shown in Figure 1 which illustrates the relation between the applied load and the displacement at the top of the column.

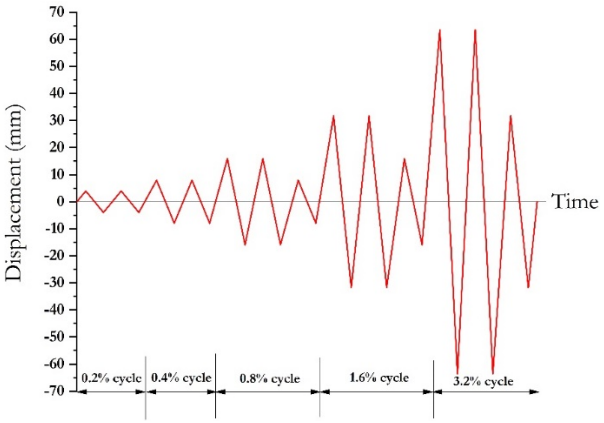

Figure 1 Lateral displacement history [26]

Description of the FE Model

In order to simulate the test in [26], a square slab portion with a central column has been modelled. In order to avoid any uncertainty in the results and because of the difference in the position of the lateral load application and displacement reading in the experimental test, spans from the experiment have been maintained in the model. Restraints were defined as roller supports at the bottom of the slab and as a pin connection at the bottom of the column according to boundary conditions addressed in the experimental test setup. The applied gravity load was simulated by uniformly distributed load of 0.007 MPa over the slab representing the lead blocks (48 each weighing 436 N on average) and a concentrated jacking force applied at the bottom in the experiment. It should be noted that this excludes self-weight of the connection which is calculated by the software, ABAQUS. The lateral load was applied as a linearly controlled cyclic displacement using a boundary condition following the protocol given in Figure 1 through amplitude definition. It was applied through a steel loading plate with material properties similar with the reinforcement bars. Details regarding the geometry and boundary conditions of the connection in the finite element models are illustrated in Figure 2.

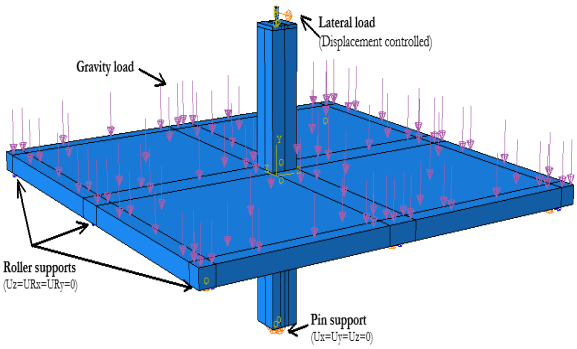

Figure 2 Simulated boundary conditions and loading of connection

CDPM incorporated in ABAQUS has been chosen for the analysis since it can describe the failure of concrete both from plastic deformation and stiffness degradation either under monotonic and cyclic loading conditions. The model was originally proposed by Drucker and Prager [27] and later modified by [28] in order to consider the evolution of

compression and tensile resistances. The model assumes that cracking and crushing are the basic failure mechanisms of concrete and it suggests the use of the principles of damage mechanics and plasticity in combination to better describe concrete behavior. Through using this model, the damage can be described through the evolution of a scalar damage variable with the inelastic deformation while plasticity with definition of a yield surface and its evolution throughout a loading procedure.

The uniaxial compressive stress-strain relationship for concrete was determined using a relationship proposed by Thorenfeldt et. al. [29]

$$\frac{f_c}{f_c'} = \frac{n(\frac{\varepsilon_c}{\varepsilon_{co}})}{(n-1)+(\frac{\varepsilon_c}{\varepsilon_{co}})^{nk}} \quad (1)$$

where, f_c is the stress at any strain ε_c, ε_{co} is the strain at maximum stress f_c' and ε_u is the strain at failure. In the above equation 'k' takes a value of 1 for the values of $\left(\frac{\varepsilon_c}{\varepsilon_{co}}\right) < 1$ and values greater than 1 for $\left(\frac{\varepsilon_c}{\varepsilon_{co}}\right) > 1$. The power 'n' can be expressed as an approximate function of the compressive strength of normal-weight concrete as $n = 0.4 \times 10^{-3} f_c'\,(psi) + 1.0$.

Figure 3 illustrates the data used in the software to model the uniaxial compressive behavior after [29].

For tensile behavior, a linear stress–strain relationship was adopted to for uncracked concrete and a nonlinear stress–crack width relationship was assumed from the study of Hordijk [30] given in Eq. (2) and illustrated in Figure 4.

$$\frac{f_t}{f_t'} = \left[1+\left(c_1 \cdot \frac{w}{w_c}\right)^3\right] \cdot exp\left(-c_2 \cdot \frac{w}{w_c}\right) - \frac{w}{w_c} \cdot (1+{c_1}^3) \cdot exp(-c_2) \quad (2)$$

where f_t is the tensile stress of concrete (MPa), f_t' is the tensile strength (MPa), w is the crack width (mm), w_c is the crack width at the complete release of stress which is given by $w_c = 5.14\frac{GF}{ft}$ (mm) and GF is the fracture energy required to create a unit area of stress-free crack given by $GF = 0.073 \cdot {f_c}^{0.18}(N/mm)$. The constants are $c_1 = 3$ and $c_2 = 6.93$.

The scalar damage variables in tension and compression were calculated using the equation presented in [31] for these variables.

Regarding the definition of plasticity, concrete behavior in CDPM depends on four constitutive parameters: dilation angle (ψ), eccentricity (ϵ), viscosity (μ), shape parameter (K_c) and the ratio of uniaxial to bi-axial compression strength (f_{bo}/f_{co}). Table 1 describes the values used in this study referring [25] and [32].

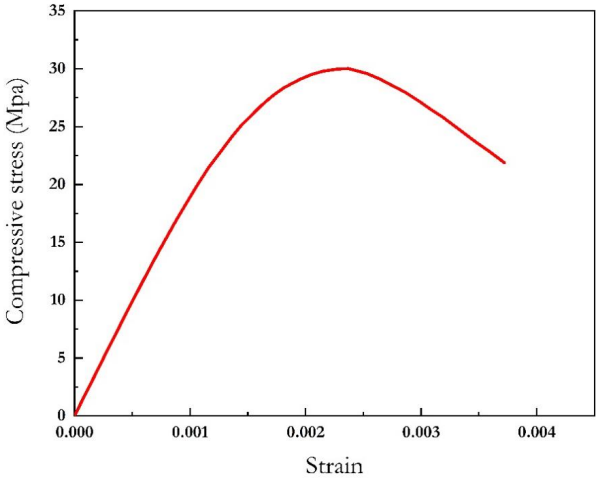

Figure 3 Material model for concrete in compression [29]

Table 1 Values of CDPM plastic parameters used [25], [32]

K_c	ψ	f_{bo}/f_{co}	ϵ	μ
0.7	36°	1.16	0.1e-05	0.00001

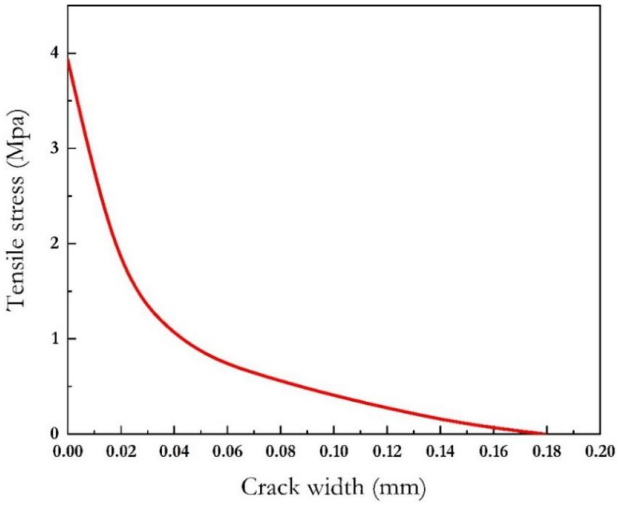

Figure 4 Material model for concrete in tension [30]

The uniaxial stress–strain relation of reinforcement was modeled as elastic with Young's modulus and Poisson's ratio of 200,000 MPa and 0.3, respectively. Plastic behavior was defined in a tabular form with a stress strain curve from [26] converted into true stress and strain values and inserted in ABAQUS in terms of yield stress and corresponding plastic strain [25]. Other than that, a combined isotropic-kinematic hardening has been used to capture the behavior under cyclic loading with calibrated parameters from [33].

A perfect bonding has been assumed to between the concrete and steel since literature have showed that acceptable results have been obtained using this kind of assumption [23]. For the finite elements, 3D 8-noded hexahedral (brick) elements having 3 degrees of freedom in each node (translations in X, Y and Z directions) were utilized for modeling concrete elements with reduced integration (C3D8R). In order to model reinforcements, 2-noded truss

elements (T3D2) having 3 degrees of freedom in each node (translations in X, Y and Z directions of global coordinates system) were used.

As for mesh size convergence, the C3D8R elements were made to be 2 in and 3 in elements at first in the process of model validation. However, the results have shown that decreasing mesh size increases computation time while there is hardly a significant change in connection capacity. As a result, the models for the parametric study including the control specimen were all made with 3 in meshes.

Validation of FE Model

A comparison between load displacement relation of the connection namely specimen 1 in [26] and the FPC connection model in this study is given in Figure 5 and in Table 2. In these illustrations and the rest of the paper, the drift displacement is defined as relative horizontal displacement between the top and base of the column and the percentage drift is equal to the drift displacement divided by the height between top and base of column.

The results in Table 2 are peak lateral loads and drifts predicted by the numerical simulation and reported by experimental test results and it can be seen that the model is good enough to predict the two quantities. The relative error with respect to the peak lateral load is 1.5% and the relative error with respect to the ultimate drift is 2.6%. The results presented in Figure 5 and Figure 6 show force-displacement curves of the two specimens. It can be clearly see that the response of the two specimens are comparable in the whole range of loading though the experimental specimen exhibit pinching in its hysteresis curve and display a high degree of yielding while the FE models show less of the pinching phenomenon. This less pinching behavior may be from the approximate consideration of bond-slip effect due to the perfect bonding assumption used to simulate the bond between concrete and reinforcements [34].

It is also apparent from the figures that in comparison to its companion experimental test, the FEA showed a slightly stiffer initial response. This may be due to variation in consideration of some details such as microcracks from certain construction deficiencies in experiments and finite element models [35].

Table 2 Comparison of experimental and FEA peak values

Experiment by Pan and Moehle [26]		FEA	
Peak lateral load (kN)	**Ultimate drift (%)**	**Peak lateral load (kN)**	**Ultimate drift (%)**
29.45	1.54	29.00	1.58

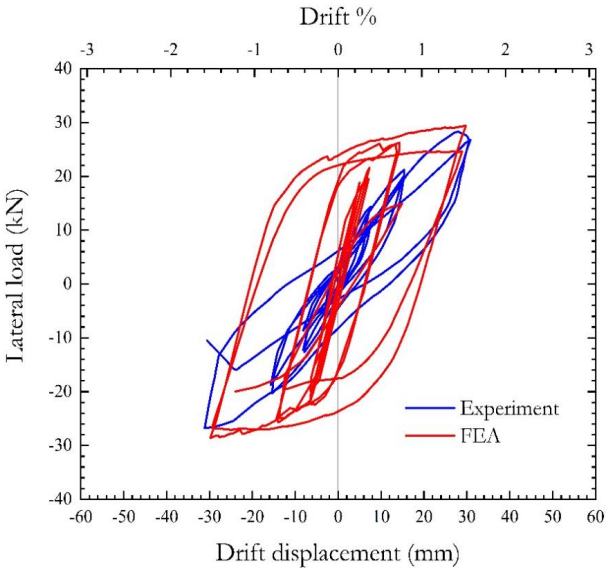

Figure 5 Comparison of load displacement hysteretic curves from experiment and FEA

Beside the quantitative comparison, the capability of the model was also checked qualitatively through the damage and crack patterns. Figure 7 gives cracking pattern reported by Pan and Moehle [26] and the tensile and compressive damages in the connection model of this paper at 1.6% drift cycle.

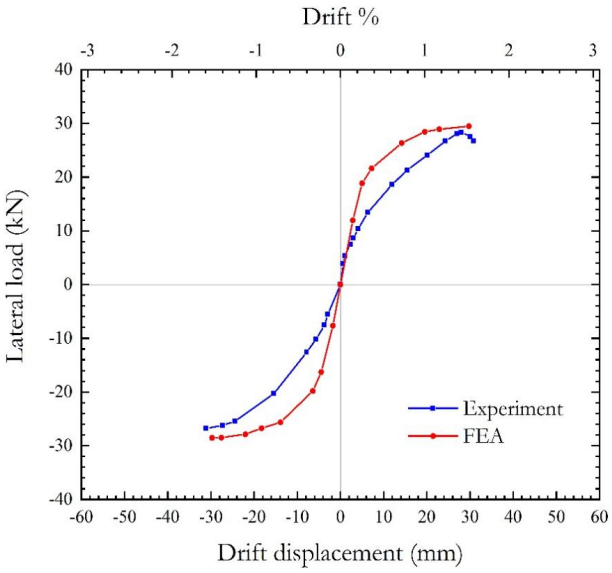

Figure 6 Comparison of load displacement envelope curves from experiment and FEA

Both experimental test and FEA resulted a specimen with punching mode of failure. This is well understood by looking the circumferential cracks on the tension face of the slab around the column in both tests at failure (Figure 7 (a) and (b)). This was also supplemented by the compression damage (Figure 7 (c)) and bulging (Figure 7 (d)) in the connection area. Judging from the patterns in Figure 7 (a) and (b) it could be argued that the model is valid to be used for subsequent studies as it predicts the overall damage on the slab well enough.

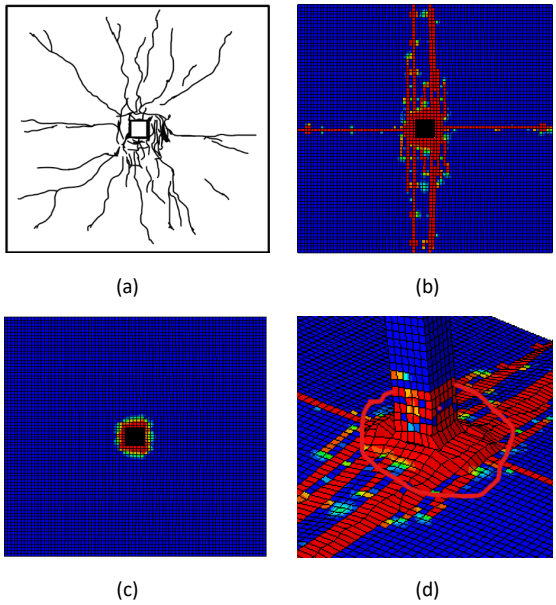

Figure 7 Illustration of punching failure in FE and experimental tests for verification

3.0 PARAMETRIC STUDY

Parametric study program

Once the FE model was validated, many alterations can be made on the control specimen to deeply understand the behavior of reinforced concrete FPC connections under lateral loads. The modifications made in this paper are on the geometry of the central column and on the surface of the plate making service openings of different size, location and shape. The control model is the connection model used in validation of the constitutive material models.

The six isolated connection models to analyze the effect of column geometry (Figure 8) are named using letters and numbers in three categories.

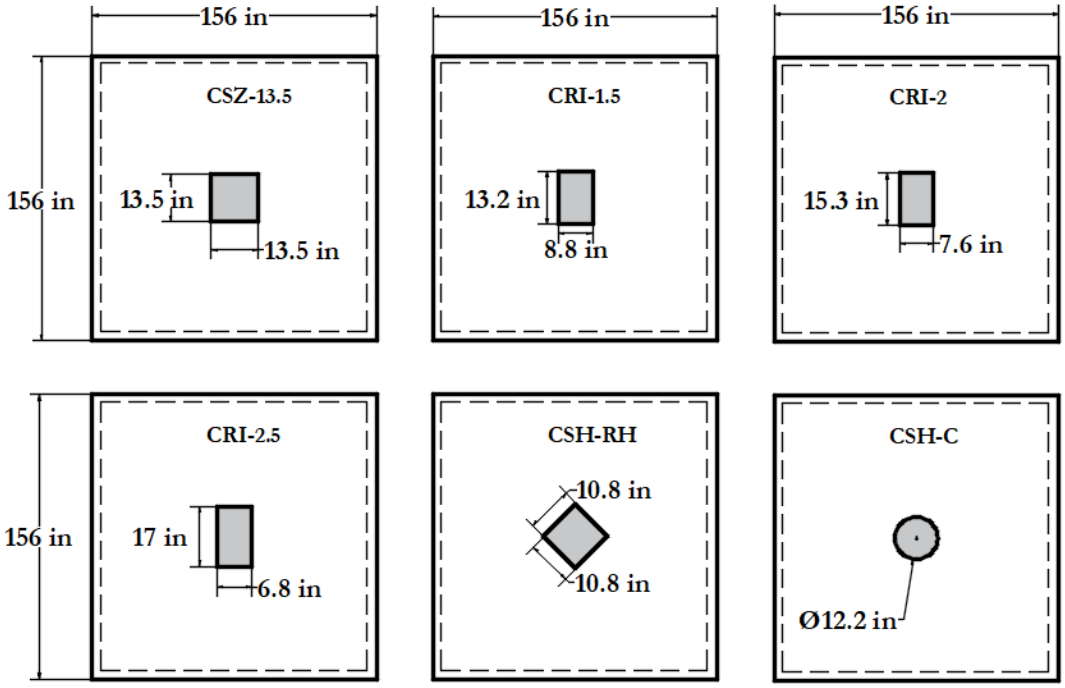

Figure 8 Schematic drawing of specimens for the effect of column size and shape (1 in = 25.4 mm)

The first letter (C) stands for column in order to show that the specimens are intended to show the effect of column geometry. The letters after are for the specific modification made in order to show specific effect intended to show: SZ stands for size, RI stands for rectangularity index and SH stands for shape. So, the dimensions of the column were increased keeping it a square, the ratio of the longest side to shortest side in cross section of the column was made above one and the cross-sectional shapes of the columns were altered in order. The letters and numbers after the hyphen are to indicate the intended feature in each class: RH stands for rhombus, C stands for circular, and the numbers are the rectangularity ratios and column dimension.

The models constructed from the control model to study the effect of service openings are comprised of connections with openings of different shapes, three distinct sizes, from three different zones and two types of arrangement on the plate surface. The opening shapes considered were a square designated as S and a circle designated C.

For square columns, three different sizes were used. The first of these sizes considered was a width of 9 in (228.6 mm), representing the limit suggested in ACI 318-05 [36] for areas on intersections of column strips, designated S. The other sizes are M, a square opening with a width similar with the width of the square column (10.8 in = 274.3 mm) and a width of 18 in (457.2 mm), representing the code recommendation for areas on the intersection of field and column strips, named here L. The locations of the openings were designated as 1, 2 or 3 as in Figure 9 after [37]. The two arrangements used were a single opening (S) and a double opening arrangement around the central column (D).

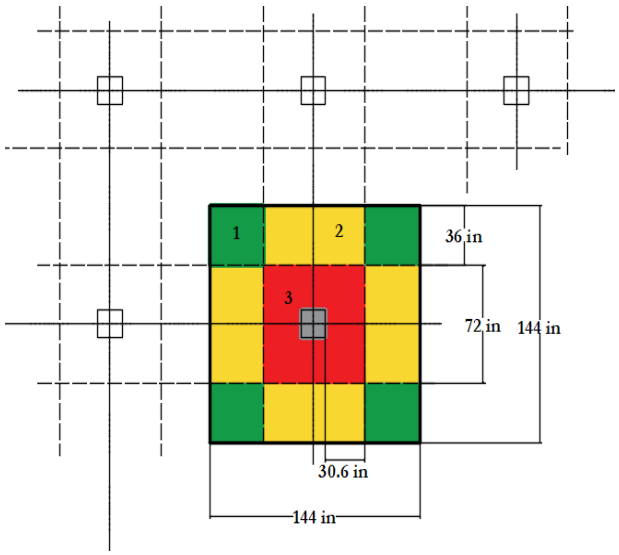

Figure 9 Possible locations for openings in specimen under study (1 in = 25.4 mm) [37]

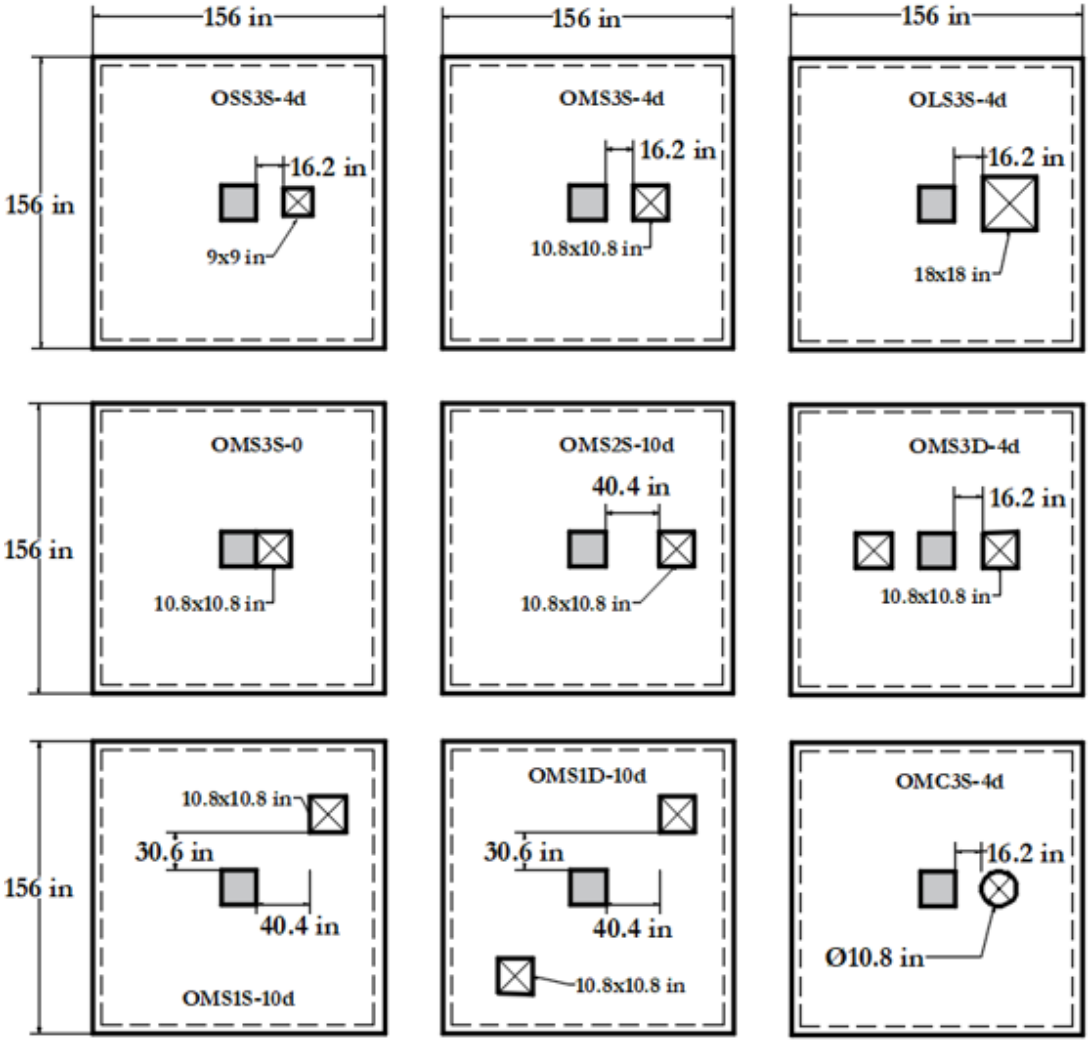

Figure 10 Schematic drawing of specimens for study of opening effect (1 in = 25.4 mm)

The labelling of specimens was in the order of size, shape, location, arrangement and a longitudinal distance from the face of central column while the first letter stands for opening. For example, a specimen labelled OMS3S-4d is an opening

with the size of the central column, square in shape, located at region 3, single by arrangement and 4d (16.2 in = 411.5 mm) from the face of the column. Beside the openings the other connection dimensions were kept constant and additional reinforcement equivalent to that interrupted by the openings was placed around the openings in all (Figure 10).

Finally, the results from the connections were compared in terms of stiffness, ductility and energy dissipation capacity of FPC connections under uniaxial lateral loads. Stiffness is an indicator of the response of a specimen during a cycle and extent of strength degradation from cycle to cycle. It is calculated as the slope of the line joining the peak of positive and negative capacity at a given cycle. The slope of this straight line is the stiffness of the assemblage corresponding to that particular amplitude. The effect of the different parameters on the stiffness degradation in laterally loaded FPC connections may be evaluated by comparing stiffness vs. drift plots. The ductility, which is of displacement, is a quantity derived by dividing the ultimate displacement (D_u) to the yield displacement (D_y). The load–displacement envelope for each specimen was used to define the yield and ultimate displacement combining the methods used by Shannag and Alhassan [38] and the method used by Pan and Moehle [10] as illustrated in Figure 11. In Figure 11, the subscripts 1 and 2 refer the loads and displacements in positive (loading) and negative (unloading) directions respectively. The ultimate displacement and displacement at first yield for ductility calculation are the averages of the respective quantities in these directions.

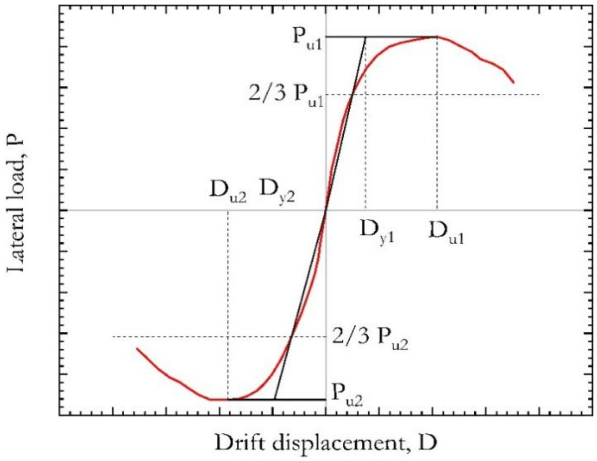

Figure 11 Definition of displacement ductility [38] and [10]

The capacity of the connections to dissipate energy is another property to describe the ability of the connections to resist lateral loads. The energy dissipation can be measured from the area of hysteresis loop. The cumulative energy dissipated which is used in this paper is for certain amplitude is summation of the dissipated energy from the start of the test up to that specific amplitude. The plots of this cumulative energy dissipation versus drift are the ones used for discussion of the effects.

Influence of Column Geometry

The first thing considered in this paper is the size of column and it was found out that that increasing the side length of a square column to 342.9 mm (13.5 in) from 274.3 mm (10.8 in) increases the load carrying capacity by 46.8% and decreases the drift capacity by 0.3% (Table 3). The trend can be clearly seen from Figure 12. stiffness of the later specimen degraded much faster than the earlier one although it was the later specimen which has higher stiffness at the start. The energy dissipated by the larger column size specimen was also larger throughout the loading. Taking into consideration the reduction in ductility by a small amount (0.4%) the specimen with the larger capacity performs better than the smaller one. However, this needs additional data since the comparison in this report is based on only two specimens.

Table 3 Summary of capacity values for column effect series

Specimens	Peak lateral load (kN)	Ultimate drift (%)	Displacement ductility	Cumulative energy dissipation (kN-mm)
Control	27.69	1.540	2.80	5474.86
CSZ-13.5	40.65	1.535	2.79	7256.68
CRI-1.5	25.10	1.537	2.94	4421.14
CRI-2	22.80	1.502	1.90	4519.64
CRI-2.5	19.72	1.504	1.86	4085.61
CSH-C	26.79	1.540	2.26	4373.69
CSH-RH	29.74	1.539	1.95	4652.75

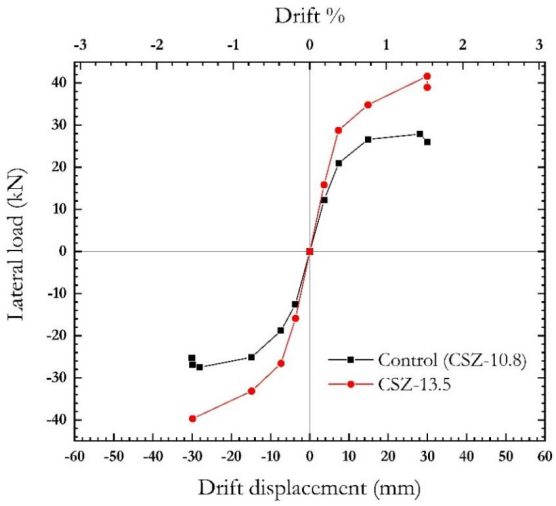

Figure 12 Lateral load versus drift envelop curves for CSZ series

The influence of column rectangularity index was deduced from the models in CRI series. The load-deflection curves for the control model (CRI-1) and variations CRI-1.5 and CRI-2 are shown in Figure 13.

With the increase of rectangularity index, both the load carrying capacity and drift capacities will decrease. In fact, increasing the rectangularity index to 2.5 from 1 have resulted a decrease in load carrying capacity by 29% and the drift capacity by 2.4% (Table 3). It can be also concluded that the increase in cumulative energy in specimens with lower RI is becomes larger and larger through cycles that the higher ones and generally the chance of the lower RI connections to

dissipate energy, resist deformation and undergo large deformation is greater.

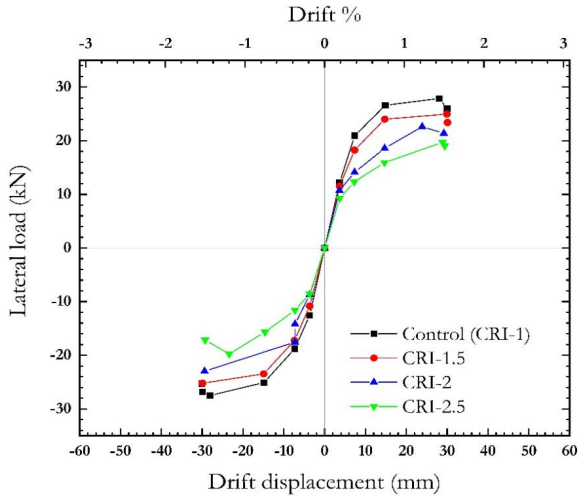

Figure 13 Lateral load versus drift envelop curves for CRI series

It was also observed that a circular column will tend to decrease the lateral load carrying capacity while the rhombus shape increases this capacity relative to a square column of identical cross-sectional area. The drift capacity, however; is maintained similar as shown in Figure 14. From the comparison of secondary variables, it can be concluded that it is the specimen with square column which stand out to be better since it got good energy dissipation capacity, a well-maintained stiffness degradation and highest ductility.

Influence of Service Openings

The first three (OSS3S-4d, OMS3S-4d and OLS3S-4d) of the nine connection models in Figure 10, referred here as OSZ series are to be compared for the effect of opening size while the next five (from OMS3S-0 to OMS1D-10d) referred as OLA series are to investigate the effect of opening location and arrangement. The other (OMC3S-4d) or OSH series is to study the effect of opening shape.

Beside the quantitative comparison, the capability of the model was also checked qualitatively through the damage and crack patterns. Figure 7 gives cracking pattern reported by Pan and Moehle [26] and the tensile and compressive damages in the connection model of this paper at 1.6% drift cycle.

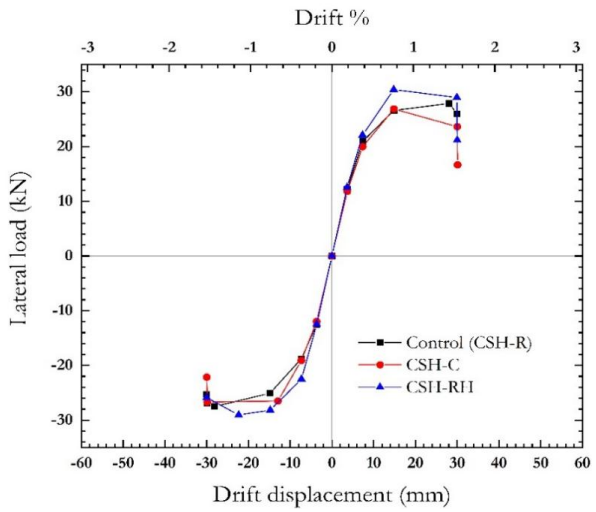

Figure 14 Lateral load versus drift envelop curves for CSH series

Although a significant difference has not been discovered in load and drift capacity related to the effect of opening size, the energy dissipation capacity and ductility decrease with the increasing of opening size (Figure 15 and Table 4). Making openings as large as the column size is not as bad as suggested in the codes although this also needs further investigation.

Figure 16 shows the load-displacement envelope curves of the specimens for the effect of opening distance, location and arrangement. Making openings near the column will result in lower stiffness and cumulative energy dissipated throughout the lateral loading cycles, but the effect weakens as the distance increases. In addition, the ductility was found to be proportional to the distance of opening from the face of column (Table 4). So, it can be concluded that placing an opening near the column does not do good.

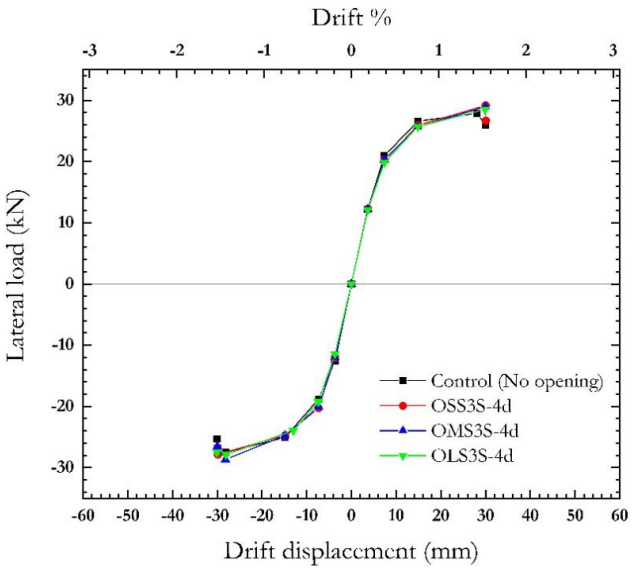

Figure 15 Lateral load versus drift envelop curves for OSZ series

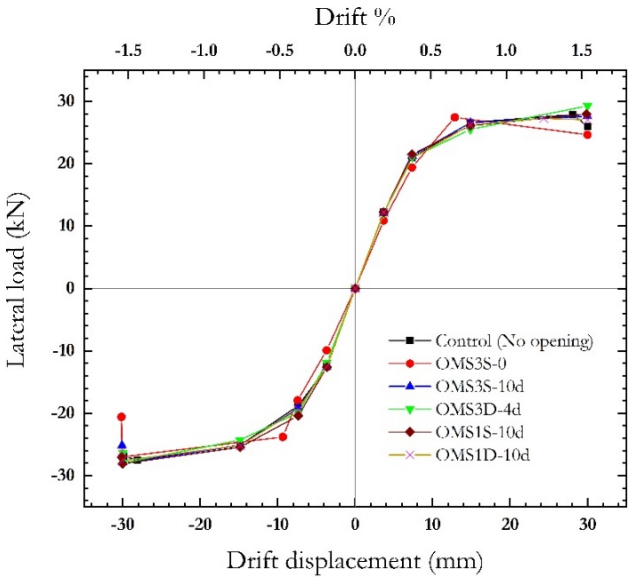

Figure 16 Lateral load versus drift envelop curves for OSA series

Table 4 Summary of capacity values for opening effect series

Specimens	Peak lateral load (kN)	Ultimate drift (%)	Disp. ductility	Cumulative energy dissipation (kN-mm)
Control	27.69	1.540	2.80	5474.86
OSS3S-4d	28.51	1.538	2.94	5274.89
OMS3S-4d	28.83	1.537	2.80	5239.57
OLS3S-4d	28.21	1.536	2.76	5200.86
OMS3S-0	27.22	1.542	1.97	3426.63
OMS2S-10d	27.79	1.539	3.03	5417.38
OMS3D-4d	28.61	1.537	2.95	5212.38
OMS1S-10d	28.04	1.536	3.13	5320.84
OMS1D-10d	27.43	1.539	2.77	5380.35
OMC3S-4d	28.08	1.539	2.17	5437.73

Finally, placing multiple openings or making circular openings rather than square shape have resulted in degradation of performance by some amount (Table 4, Figure 16 and Figure 17).

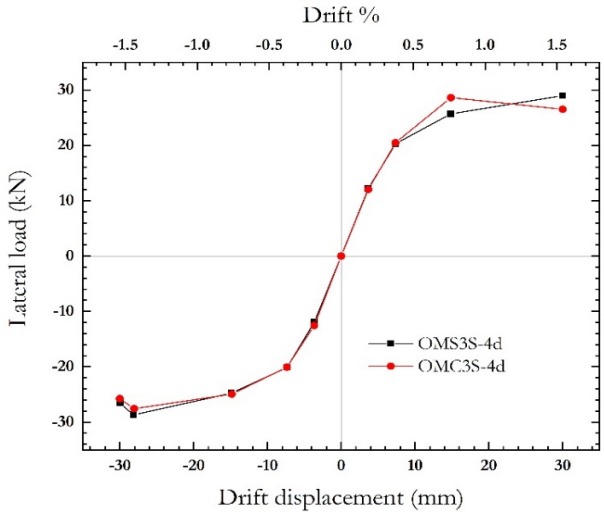

Figure 17 Lateral load versus drift envelop curves for OSH series

4.0 CONCLUSION

The current study is concerned with the lateral load behavior of internal reinforced concrete flat plate connections without transverse reinforcement. In order to understand the lateral load response of these systems and the effect of some variables, a FEA is performed with models of a scaled down connection loaded under gravity and reverse cyclic loading using general purpose finite element software ABAQUS. After analysis of the finite element connection models, certain conclusions have been made.

The concrete damage plasticity model gives good approximation in load carrying and drift capacity of flat plate connections under lateral loads. However, the pinching in hysteresis loops observed during experimental tests could not be captured. It may need to use other constitutive models or consider the bond-slip behavior between the concrete and steel reinforcements. This may constitute the object of future studies.

The effect of column geometry can be interpreted in different ways. To begin with, with the increase of rectangularity index, it can be concluded that both the lateral load carrying and drift capacities decrease. Besides, the chance of the lower RI connections to dissipate energy, resist deformation and undergo large deformation was also found generally greater.

Furthermore, it was also observed that a circular column will tend to decrease the lateral load carrying capacity while the rhombus shape increases it relative to a square column of identical cross-sectional area. The drift capacity, however; was maintained uniform. From the comparison of secondary variables, it can be concluded that it is the specimen with square column which stand out to be better since it got good energy dissipation capacity, a well-maintained stiffness degradation and highest ductility. However, this needs additional data since the comparison in this report is based on only two models.

The analysis for the effect of service openings on the flat plate has also revealed some conclusions.

Although a significant difference in load carrying capacity has not been discovered related to the effect of opening size, the energy dissipation capacity and ductility decrease with the increasing of opening size. So, making openings as large as the column size may not be as bad as it seems in literature even if it needs further investigation with more samples.

On the other hand, placing an opening near the column does not do good. Making openings near the column resulted in lower stiffness and cumulative energy dissipation throughout the lateral loading cycles. The effect weakens as the distance increases. In addition, the ductility was found to be proportional to the distance of opening from the face of column. Finally, placing multiple openings or making circular openings rather than square shape will degrade the performance by some amount.

Acknowledgement

The authors would like to thank Addis Ababa Science and Technology University for partially funding this research.

References

[1] M. G. Sahab, A. F. Ashour, and V. V. Toropov, 2005. "Cost optimisation of reinforced concrete flat slab buildings," *Engineering Structures*, 27(3): 313-322, https://doi.org/10.1016/j.engstruct.2004.10.002

[2] D. N. Farhey, M. A. Adin, and D. Z. Yankelevsky, 1993."RC flat slab-column subassemblages under lateral loading," *Journal of Structural Engineering*, 119(6): 1903-1916 https://doi.org/10.1061/(ASCE)0733-9445(1993)119:6(1903)

[3] M. B. D. Hueste and J. K. Wight, 1999. "Nonlinear Punching Shear Failure Model for Interior Slab-Column Connections," *Journal of Structural Engineering,* 125(9): 997-1008. https://doi.org/10.1061/(ASCE)0733-9445(1999)125:9(997)

[4] S. King and N. J. Delatte, 2004. "Collapse of 2000 Commonwealth Avenue: Punching Shear Case Study," *Journal of Performance of Constructed Facilities*, 18(1): 54-61. https://doi.org/10.1061/(ASCE)0887-3828(2004)18:1(54)

[5] W. Y. Kam and S. Pampanin, 2011."The seismic performance of RC buildings in the 22 February 2011 Christchurch earthquake," *Structural Concrete.*, *12*(4): 223-233 https://doi.org/10.1002/suco.201100044

[6] N. W. Hanson and J. M. Hanson, 1968.Shear and moment transfer between concrete slabs and columns. Portland Cement Association, Research and Development Laboratories

[7] S. Islam and R. Park, 1976."Tests on slab-column connections with shear and unbalanced flexure," *Journal of Structural Division*, 102(3): 549-568, https://doi.org/10.1061/JSDEAG.0004296

[8] W. Dilger, M. Z. Elmasri, and A. Ghali,1978."Flat Plates with Special Shear Reinforcement Subjected to Static Dynamic Moment Transfer," *ACI Journal Proceedings*, 75(10): 543-549 https://doi.org/10.14359/10967

[9] J. P. Moehle and J. W. Diebold, 1985."Lateral load response of flat-plate frame," *Journal of Structural Engineering*, 111(10): 2149-2164 https://doi.org/10.1061/(ASCE)0733-9445(1985)111:10(2149)

[10] A. Pan and J. P. Moehle, 1989. "Lateral displacement ductility of reinforced concrete flat plates," *Structural Journal,* 86(3): 250-258 https://doi.org/10.14359/2889

[11] A. D. Pan and J. P. Moehle, 1992."An experimental study of slab-column connections," *Structural Journal*, 89(6): 626-638. https://doi.org/10.14359/4133

[12] I.-S. Drakatos, A. Muttoni, and K. Beyer, 2016. "Internal slab-column connections under monotonic and cyclic imposed rotations," *Engineering Structures,* 123: 501-516, https://doi.org/10.1016/j.engstruct.2016.05.038

[13] B. Isufi, A. Pinho Ramos, and V. Lúcio, 2019, "Reversed horizontal cyclic loading tests of flat slab specimens with studs as shear reinforcement," *Structural Concrete,* 20(1): 330-347.doi: https://doi.org/10.1002/suco.201800128

[14] B. Isufi, I. Cismasiu, R. Marreiros, A. P. Ramos, and V. Lúcio, 2020."Role of punching shear reinforcement in the seismic performance of flat slab frames," *Engineering Structures,* 207: 10238. https://doi.org/10.1016/j.engstruct.2020.110238

[15] S. Teng, H. K. Cheong, K. L. Kuang, and J. Z. Geng, 2004. "Punching shear strength of slabs with openings and supported on rectangular columns," *Structural Journal*, 101(5): 678-687, https://doi.org/10.14359/13390

[16] Y. T. and S. Teng, 2005. "Interior Slab-Rectangular Column Connections Under Biaxial Lateral Loadings," *ACI Special Publication*, 232: 147-174. https://doi.org/10.14359/14941

[17] J. Sagaseta, L. Tassinari, M. Fernández Ruiz, and A. Muttoni, 2014. "Punching of flat slabs supported on rectangular columns," *Engineering Structures,* https://doi.org/10.1016/j.engstruct.2014.07.007

[18] A. Essa, 2003."Punching of high strength concrete flat plates with openings." PhD Thesis, Cairo University,

[19] A. Sherif, G. Ghanem, and A. Abdel-Razek, 2006, "Punching Shear Strength of Interior Flat-Slab Connections with Openings," in *1st International Structural Specialty Conference, ISSC-1, Canadian Society for Civil Engineering Annual Conference, Calgary, Canada,* May, 23-26.

[20] L. L. J. Borges, G. S. Melo, and R. B. Gomes, 2013."Punching Shear of Reinforced Concrete Flat Plates with Openings.," *ACI Structural Journal,* 110(4). https://doi.org/10.14359/51685740

[21] D. C. Oliveira, R. B. Gomes, and G. S. Melo, 2014. "Punching shear in reinforced concrete flat slabs with hole adjacent to the column and moment transfer," *Revista IBRACON Estruturas e Materiais,* 7(3): 414-467, https://doi.org/10.1590/S1983-41952014000300006

[22] R. B. Gayed and A. Ghali, 2008. "Unbalanced Moment Resistance in Slab-Column Joints: Analytical Assessment," *Journal of Structural Engineering*, 134(5): 859-864. https://doi.org/10.1061/(ASCE)0733-9445(2008)134:5(859)

[23] A. S. Genikomsou and M. A. Polak, 2014"Finite element analysis of a reinforced concrete slab-column connection using ABAQUS," In Structural Congress, 813-823, https://doi.org/10.1061/9780784413357.072

[24] A. Setiawan, R. L. Vollum, and L. Macorini, 2019 "Numerical and analytical investigation of internal slab-column connections subject to cyclic loading," *Engineering Structures,* 184: 535-554. https://doi.org/10.1016/j.engstruct.2019.01.089

[25] D. Systèmes, 2007."Abaqus analysis user's manual," Simulia Corp. Provididence, RI, USA,

[26] A. P. Pan and J. P. Moehle, 1988. "Reinforced concrete flat plates under lateral loading: an experimental study including biaxial effects," 88(16). Earthquake Engineering Research Center, University of California at Berkeley

[27] D. C. Drucker and W. Prager, 1952 "Soil mechanics and plastic analysis or limit design," Quarterly of Applied Mathematics, 10(2): 157-165. https://doi.org/10.1090/qam/48291

[28] J. Lee and G. L. Fenves, 1998. "A plastic-damage concrete model for earthquake analysis of dams," *Earthquake Engineering and Structural Dynamics,* 27(9): 937-956. https://doi.org/10.1002/(SICI)1096-9845(199809)27:9<937:AID-EQE764>3.0.CO;2-5

[29] E. Thorenfeldt, " 1987."Mechanical properties of high-strength concrete and applications in design

[30] D. A. Hordijk, 1992."Tensile and tensile fatigue behaviour of concrete; experiments, modelling and analyses," *Heron, 37*(1)

[31] J. Lubliner, J. Oliver, S. Oller, and E. Oñate, 1989. "A plastic-damage model for concrete," *International Journal of Solids and Structures,* 25(3): 299-326. https://doi.org/10.1016/0020-7683(89)90050-4

[32] P. Kmiecik and M. Kaminski, 2011. "Modelling of reinforced concrete structures and composite structures with concrete strength degradation taken into consideration," *Archives Of Civil And Mechanical Engineering*, 11(3): 623-636. https://doi.org/10.1016/S1644-9665(12)60105-8

[33] P. Krolo, D. Grandić and Ž. Smolčić, 2016"Experimental and numerical study of mild steel behaviour under cyclic loading with variable strain ranges," *Advances in materials science and engineering*. https://doi.org/10.1155/2016/7863010

[34] B. Alfarah, 2017."Advanced computationally efficient modeling of RC structures nonlinear cyclic behavior,"

[35] M. A. Najafgholipour, S. M. Dehghan, A. Dooshabi, and A. Niroomandi, 2017"Finite element analysis of reinforced concrete beam-column connections with governing joint shear failure mode," *Latin American Journal Solids and Structures*, 14(7): 1200-1225. https://doi.org/10.1590/1679-78253682

[36] ACI Committee, 2005."Building code requirements for structural concrete (ACI 318-05) and commentary (ACI 318R-05)," American Concrete Institute

[37] A. Newman, 2001. P.E. Structural renovation of buildings: Methods, details, and design examples. McGraw-Hill Education, New York, USA

[38] M. J. S. and M. A. Alhassan, 2005. "Seismic Upgrade of Interior Beam-Column Sub-assemblages with High-Performance Fiber-Reinforced Concrete Jackets," *ACI Structural Journal*, 102(1): 131. https://doi.org/10.14359/13538